Determination of aerodynamic damping and force coefficients of filleted twin cables in dry conditions through passive-dynamic wind tunnel tests

Emanuele Mattiello[1], Mads B. Eriksen[1] and Christos T. Georgakis[2]

[1]FORCE Technology, Hydro- and Aerodynamics, Kgs. Lyngby, DK.

emmi@force.dk

[2]Department of Civil Engineering, Technical University of Denmark (DTU), Kgs. Lyngby, DK.

Abstract

Moderate amplitude vibrations continue to be reported on the Øresund Bridge cables, although fitted with fillets and dampers. To further investigate the aerodynamics of the bridge's twin-cable arrangement, 1:2.3 scale passive-dynamic wind tunnel tests of the cables were performed at the DTU/FORCE Technology Climatic Wind Tunnel facility. The measured aerodynamic damping of the twin-cable arrangement in dry conditions was compared to the values obtained from full-scale monitoring and from an analytical model using static force coefficients. The comparison revealed broad agreement in the investigated Re range, as did the force coefficients obtained from dynamic and static tests.

1 Introduction

Although widely researched over the last two decades, bridge cable vibrations remain a problem for bridge designers and operators. The approach followed to minimize these vibrations has generally been twofold. Helical fillets or dimples have been applied on the cables surface to change their aeroelastic behaviour, whilst mechanical dampers have been added to increase energy dissipation.

The cable-stayed Øresund Bridge, linking Denmark and Sweden, was one of the first bridges to incorporate this dual approach with double helical fillets and dampers. Nevertheless, vibrations of the cables have been observed since before its opening in 2000. More recently, Acampora & Georgakis (2011) reported moderate vibration incidences in both dry and wet conditions for skewed winds. Various mechanisms may be responsible for the reported vibrations, including rain-wind-cable interaction and dry inclined galloping.

The flow around circular cylinders positioned close to each other differs from the flow around a single circular body, because the cylinders respond differently depending on the angle of attack of the incoming flow and the mutual spacing between the cylinders. For twin cables aligned in the vertical direction, the mean horizontal wind sees the stays in a side-by-side configuration for which proximity interference occurs (Zdravkovich, 2003). In the case of the Øresund Bridge, the spacing to diameter ratio, S/D=2.68, leads to a normal to cable plane flow pattern which falls within the coupled wakes regime (Zdravkovich, 2003), where the gap between the cables is sufficiently large for two parallel vortex streets to form. Proximity interference effects may lead to various modes of synchronization in the vortex formation and shedding process. This means that both cables undergo vortex shedding at the same frequency, in-phase or out-of-phase (Sumner, 2010). On full-scale bridges, inclined stays may often be subjected to a yawed wind action, which also generates an axial flow. This interferes with the regular von Kármán vortex shedding and, for coupled cylinders, with the gap flow as well. Raeesi *et al.* (2012) found that for a certain cable-wind angle range, the symmetry and the characteristics of the flow field are altered and negative aerodynamic damping may occur. Also the regular von Kármán vortex shedding could be suppressed, leading to limited-amplitude oscillations.

In addition, the presence of surface modifications makes the flow-structure interaction even more complex, e.g. helical fillets change the flow by creating a separation point which varies along the cable surface (Kleissl & Georgakis, 2012).

The Øresund Bridge cable arrangement was originally studied by Larose & Smitt (1999), and its aerodynamic damping was recently estimated from full-scale measurements using an output-only modal analysis employing Stochastic Subspace Identification (SSI) (Georgakis & Acampora, 2011) as well as an Eigenvalue Realisation Algorithm (ERA), as reported by Acampora *et al.* (2012). Static wind tunnel tests of this twin-cable arrangement have also been undertaken by Acampora & Georgakis (2013).

To further investigate the aerodynamics of the Øresund Bridge twin cables, a series of passive-dynamic wind tunnel tests has been conducted in both dry and wet conditions. This paper presents the investigation in dry conditions.

2 Wind Tunnel Tests

2.1 Test Facility

Experimental investigations were carried out in the closed-circuit DTU/FORCE Technology Climatic Wind Tunnel (Georgakis *et al.*, 2009), in Kgs. Lyngby, Denmark. The tests were performed in smooth flow, with a turbulence intensity of less than 1% in the flow direction measured in the closed 2m×2m×5m test section.

2.2 Cable Model

A 1:2.3 scale section-model of the twin-cable arrangement was produced using PVC piping with outer diameter D=110mm and thickness t=6mm. Two pipes of 3.05m length were rigidly linked together to produce the model shown in Figure 2.1. The mass of the model was m=28.3kg. Full-scale monitoring of the bridge cables (Acampora, 2011), revealed several vibration incidences up to 1D at the cable mid-span for the geometrical configuration with cable inclination θ=30° and horizontal cable-wind yaw angle β=70°. Figure 2.2 shows the cable-wind angle convention. The identified configuration was chosen for the subsequent test campaign and reproduced in the test set-up, see Figure 2.1. The geometrical configuration of the twin-cable model and its size led to a blockage coefficient b_k=12.6%. This blockage was accepted to avoid further scaling of the helically filleted twin-cable model. To reproduce the surface roughness, the pipes were treated with sand paper. A scaled double helical fillet was then wrapped around the two pipes of the model.

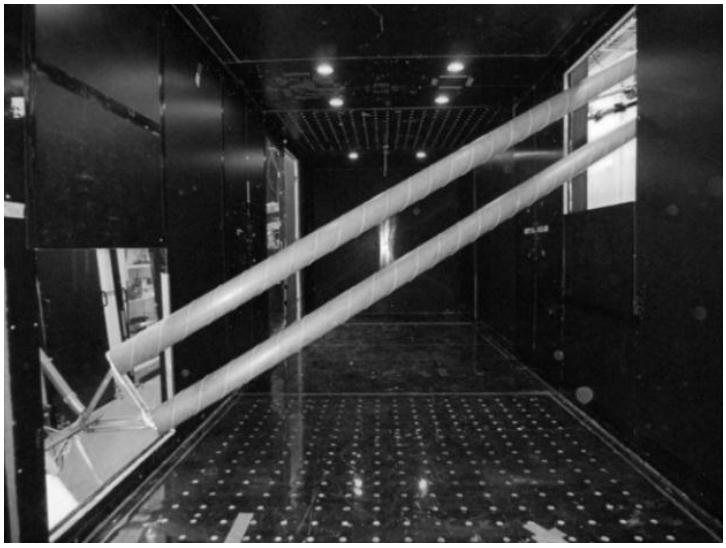

Figure 2.1: Downstream view of the twin-cable model mounted on the passive-dynamic rig.

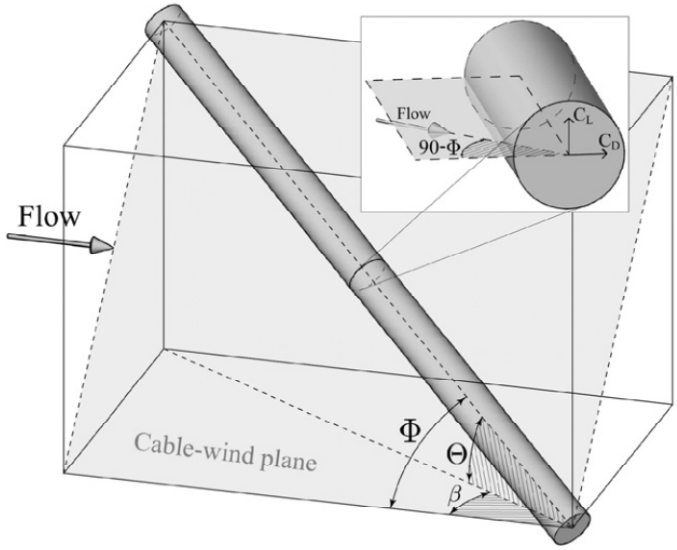

Figure 2.2: Cable-wind angle convention showing the definition of drag and lift coefficients.

2.3 Dynamic Rig

A two degree-of-freedom (2DoF) dynamic rig was designed to allow motion of the model in the two principal directions, out-of-plane and in-plane, both perpendicular to the model axis. A single in-plane spring and two horizontal out-of-plane springs supported the model at each end, see Figure 2.3. The stiffness of the springs was adjusted in order to match the 1st in- and out-of-plane natural frequencies of the prototype cables, which according to Froude scaling corresponded to 0.86Hz and 0.85Hz respectively.

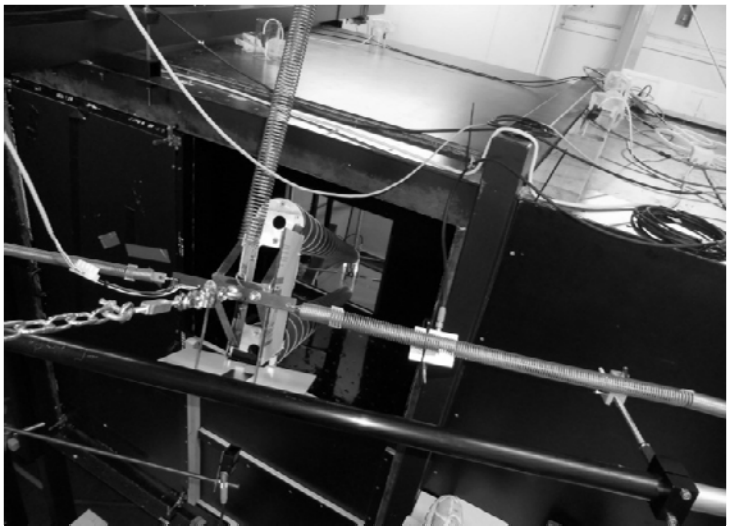

Figure 2.3: Two-degree-of-freedom dynamic rig – top end.

The test section was partially opened at the cable ends to allow attachment to the rig and movement of the section-model. The openings were designed to allow amplitudes of up to 1D and to account for the static displacement in the flow direction due to the increasing drag. The influences of the openings on velocity and turbulence intensities were investigated through flow profile measurements. The velocity was found constant through the cross-section of the tunnel excluding the first 100mm from the walls. Along the 900mm wide wall openings the velocity in the flow direction decreased by about 20% and the turbulence intensity increased with a factor of three from the upstream part to the downstream part of the opening, i.e. the model was exposed to different boundary conditions when pushed downstream due to the drag.

2.4 Test Procedure

To evaluate the damping as a function of Reynolds number, Re=DU/ν, the model was manually excited and the free-vibration decay registered using four laser displacement transducers, two per end. The tests were performed in both out-of-plane and in-plane directions for 30 steps in velocity, ranging from U=0-30m/s with 1m/s intervals.

The aerodynamic damping ratio of the cable model, ζ_a, was determined by subtracting the damping of the rig measured at zero wind velocity, ζ_s, from the total measured damping, ζ, and scaled to represent full-scale values. Following Macdonald & Larose (2006), aerodynamic damping can be described with the form:

$$\zeta_a = \frac{\mu \mathrm{Re}}{4 m \omega_n} f(\mathrm{Re}, C_D, C_L, \alpha, \phi) \tag{1}$$

For cylinders with similar aerodynamic properties, such as a full-scale bridge cable and a scaled cable model, only mass, m, and natural frequency, ω_n, vary. This requires that flow characteristics and fluid dynamic behaviour are the same, i.e. Reynolds number and dynamic viscosity of air have to remain unchanged. Hence, the resulting scaling factor depends on the mass-frequency ratio between the full-scale cable and the scaled model, such that:

$$\lambda_{\zeta a} = \frac{\zeta_{a,model}}{\zeta_{a,full}} = \frac{m_{full}\omega_{full}}{m_{model}\omega_{model}} \tag{2}$$

Force coefficients from dynamic tests were evaluated from the mean displacement time histories. The mean displacements, $\bar{x}$ and $\bar{y}$, were combined with the modal stiffness, k, to determine the aerodynamic forces acting on the model. The force coefficients were obtained normalizing the forces with the reference area, see Eqn. 3. The effective length of the model was estimated to be l_{eff}=2.58m. The drag coefficient was blockage corrected applying the 'Maskell III' method based on Cooper *et al.* (1999).

$$C_D = \frac{F_D}{½\rho U^2 A_{ref}} = \frac{\bar{x} \cdot k_{out-of-plane}}{½\rho U^2 \cdot l_{eff} 2D} \qquad C_L = \frac{F_L}{½\rho U^2 A_{ref}} = \frac{\bar{y} \cdot k_{in-plane}}{½\rho U^2 \cdot l_{eff} 2D} \tag{3}$$

3 Analytical Modelling

Further to the experiments and the full-scale monitoring, the aerodynamic damping of the cable was evaluated analytically, applying quasi-steady assumptions. To this end, the quasi-steady 1DoF model proposed by Macdonald & Larose (2006) to predict aerodynamic damping for the in- and out-of-plane directions was applied, inserting force coefficients and their derivatives with respect to Re and the wind angle of attack α, see Eqn. 4. The data used was taken from previous cross-flow static tests on a filleted twin-cable model similar to the one tested dynamically (Acampora & Georgakis, 2013).

$$\zeta_a = \frac{\mu \mathrm{Re}}{4 m \omega_n} \cos\alpha \left\{ \cos\alpha \left[C_D \left(2\sin\phi + \frac{\tan^2\alpha}{\sin\phi} \right) + \frac{\partial C_D}{\partial \mathrm{Re}} \mathrm{Re} \sin\phi - \frac{\partial C_D}{\partial \alpha} \frac{\tan\alpha}{\sin\phi} \right] \right. \tag{4}$$
$$\left. - \sin\alpha \left[C_L \left(2\sin\phi - \frac{1}{\sin\phi} \right) + \frac{\partial C_L}{\partial \mathrm{Re}} \mathrm{Re} \sin\phi - \frac{\partial C_D}{\partial \alpha} \frac{\tan\alpha}{\sin\phi} \right] \right\}$$

Additionally, the 2DoF model of Macdonald & Larose (2008) was applied to have an indication of the theoretical coupling between the two considered directions, evaluating the cross-diagonal terms of the

2×2 damping matrix. They indicated no significant coupling until Re≈$1.1 \cdot 10^5$, while for higher Re the $\zeta_{a,yx}$ term was not negligible, indicating coupling between the two modes due to the slightly detuned system, see Figure 3.1(bottom-left). As might be expected, damping estimations with the 1DoF model coincided with the diagonal terms of the damping matrix estimated with the 2DoF model, see Figure 3.1(top-left – bottom-right).

Other conventional models were applied as well for the estimation of the aerodynamic damping: in particular the drag crisis model and the Den Hartog criterion for the out-of- and in-plane directions respectively. The drag crisis model, see Figure 3.1(top-left), predicted slightly higher damping values (5% at most) and the Den Hartog criterion, see Figure 3.1(bottom-right), slightly lower values (3% at most) compared to the 1DoF model.

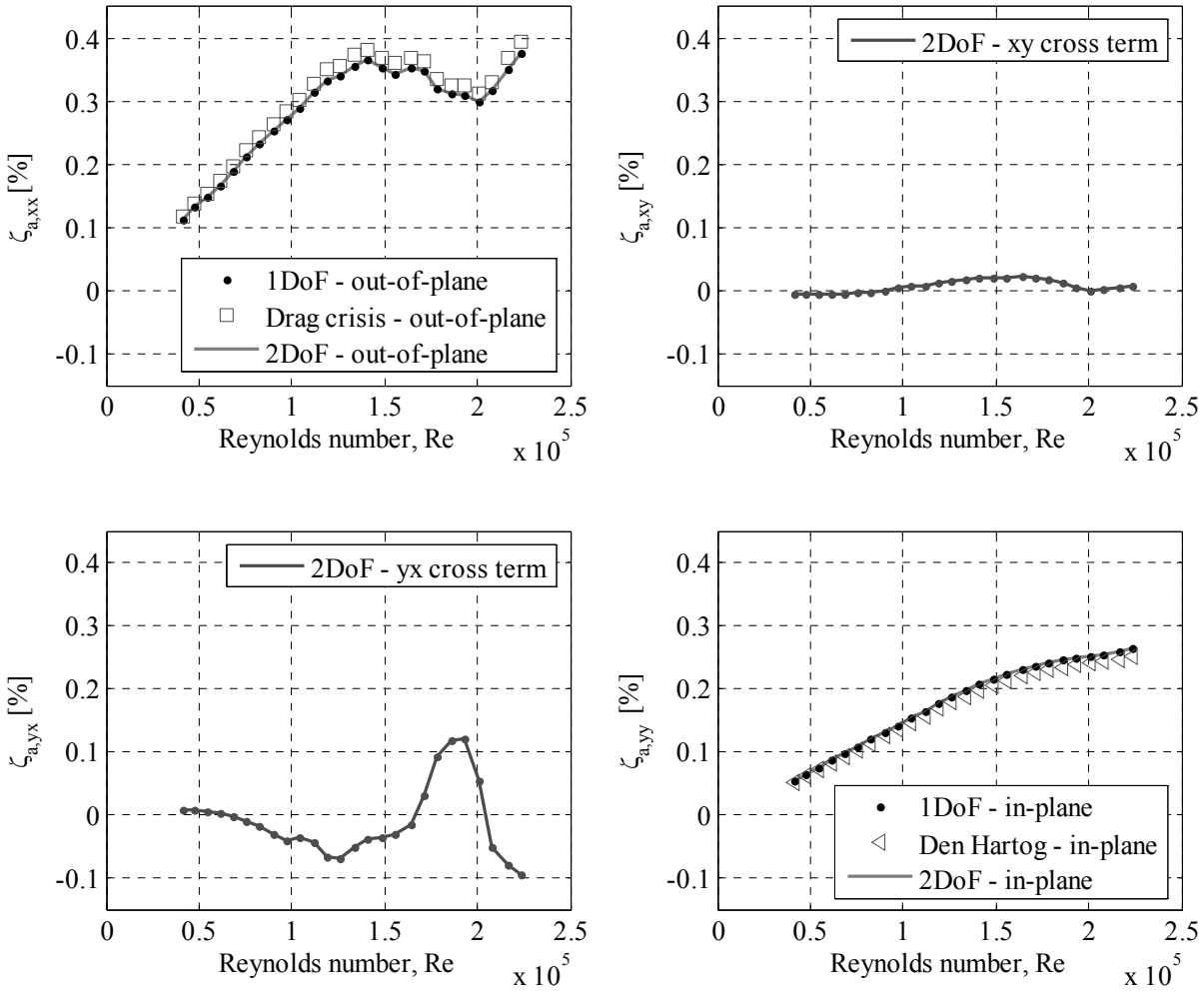

Figure 3.1: Aerodynamic damping matrix (full-scale values) determined with theoretical models using force coefficients from static cross-flow tests of a filleted twin-cable model.

4 Results and Discussion

4.1 Aerodynamic Damping

The comparison between the aerodynamic damping obtained from the dynamic tests, the values obtained from monitoring and the aerodynamic damping determined from the analytical model is shown in Figure 4.1 for the two principal directions, out-of- and in-plane. Note that dash-dotted parts of the dynamic curves represent values with a high level of uncertainty, due to the higher turbulence making the motion more unstable, see paragraph 2.3. Damping from monitoring was only available for the out-of-plane direction.

Focussing on the out-of-plane direction, Figure 4.1(left), a correlation between the three curves can be found in the subcritical Re range i.e. $Re<1.5\cdot10^5$. For higher Re, a broad agreement could be found. Overall, values of aerodynamic damping measured in the wind tunnel appeared to be $\zeta_a<0.4\%$. A decrease in aerodynamic damping was observed for all three curves from $Re=1.3\text{-}1.5\cdot10^5$ to $Re=1.8\text{-}2.0\cdot10^5$, but damping values remained positive with a minimum value of $\zeta_a=0.2\%$ and no instability was found.

The aerodynamic damping for in-plane motion is shown in Figure 4.1(right). The theoretical trend for the damping was generally reproduced by the estimation obtained from dynamic tests. Values of damping were generally below $\zeta_a<0.25\%$. The decrease in aerodynamic damping for the out-of-plane motion was not found in the in-plane motion.

An examination of the overall ratio of the damping values, revealed an approximate 2:1 ratio, confirming the theoretical prediction of in-plain damping being around half of the out-of-plane damping in the subcritical Re range, (Gimsing & Georgakis, 2012).

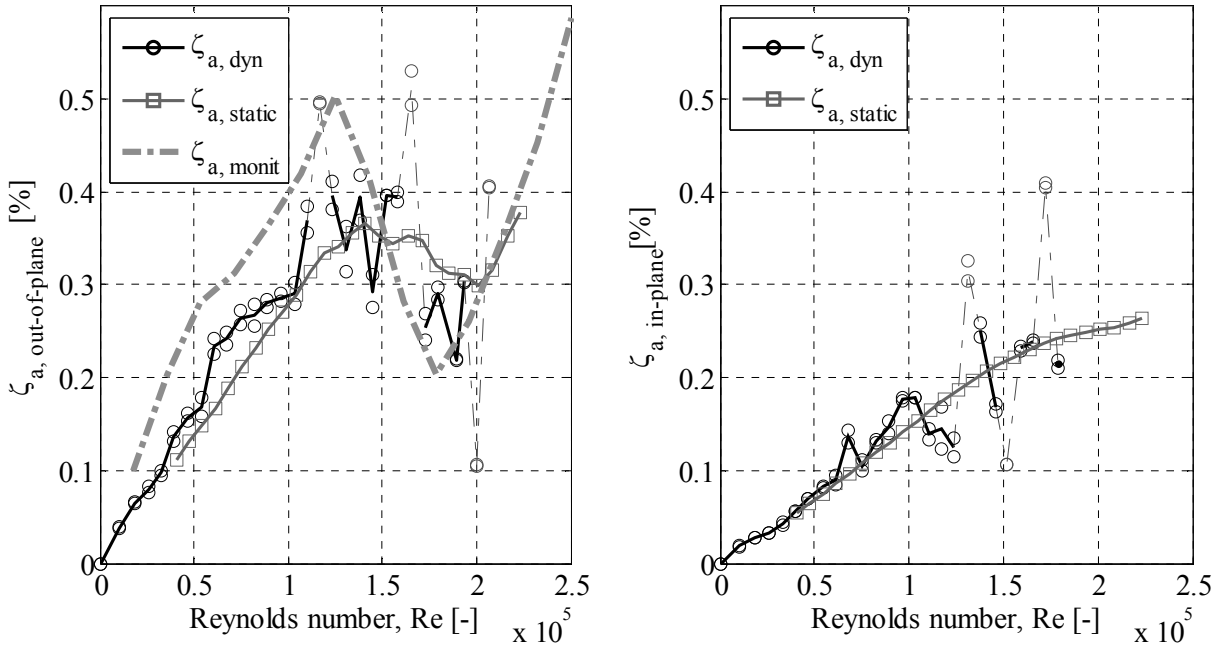

Figure 4.1: Out-of-plane (left) and in-plane (right) aerodynamic damping ratios (full-scale values) from dynamic tests, monitoring records and estimations with an analytical model.

4.2 Aerodynamic Force Coefficients

Aerodynamic force coefficients of twin cables from dynamic tests were compared to the force coefficients obtained from static tests (Acampora & Georgakis, 2013), see Figure 4.2. All coefficients are defined according to Figure 2.2.

Drag coefficients are presented in Figure 4.2(left). Note that both curves have been blockage corrected with the 'Maskell III' method. The results showed similarity in the drag variation in the Re critical range. The decrease in the drag curves at $Re\approx1.5\cdot10^5$ denoted the beginning of the critical Re range, where a decrease in the out-of-plane aerodynamic damping was also observed, see Figure 4.1(left). Generally, 'dynamic drag' appeared to be about 20% larger than static values. A possible explanation to this might be found in the differences in the set-up arrangements between dynamic and static experiments, i.e. the partially open test section of the wind tunnel, as well as the possible non quasi-steady nature of the flow around the twin cylinders when moving dynamically. Furthermore, confirmation of the applicability of the 'Maskell III' blockage correction method for dynamically tested structures has not been found in the investigated literature.

Lift coefficients are presented in Figure 4.2(right). A strong similarity was observed between the results from the two tests.

Both drag and lift coefficient agreed with previous studies on side-by-side twin cylinders. Zdravkovich (2003) shows that drag coefficient of side-by-side twin cylinders with a spacing ratio of approximately 2.6−2.7 varies between 1.2−1.3 for $0.6 \cdot 10^5 < Re < 1.6 \cdot 10^5$. Similarly, the lift varies between 0.05−0.15.

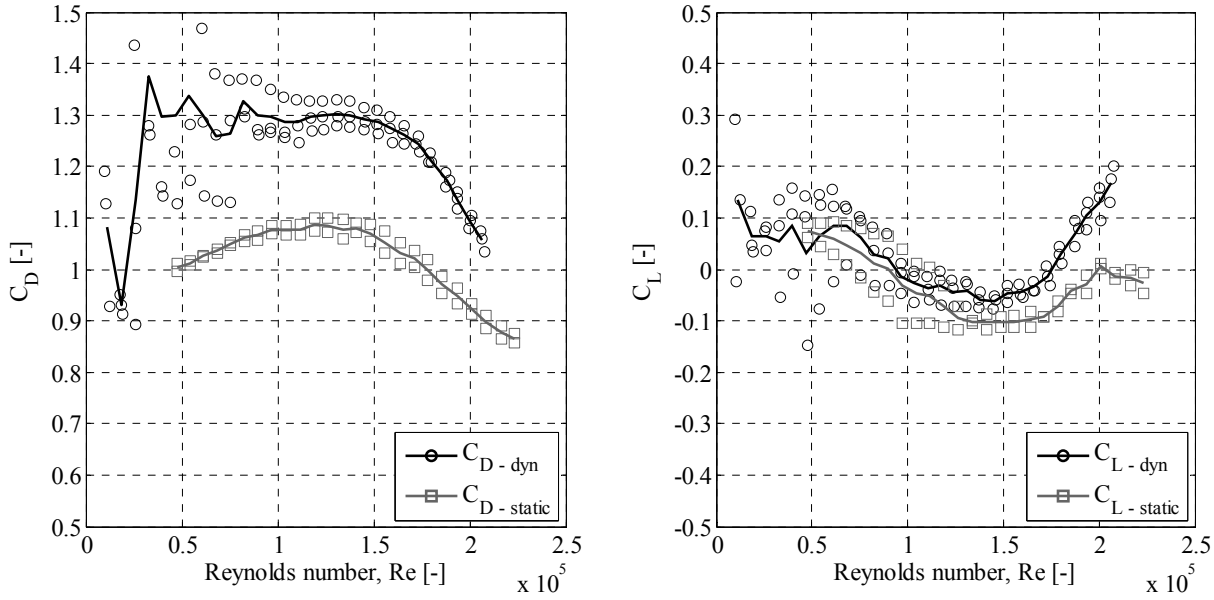

Figure 4.2: Drag (left) and lift (right) force coefficients from dynamic tests and static tests on a the twin-cable model with double helical fillet.

5 Conclusion

Passive-dynamic wind tunnel tests of a scaled section-model of the Øresund Bridge cables were performed in dry conditions to estimate aerodynamic damping and force coefficients for a specific twin-cable arrangement. The results were compared with results obtained from analytical models using static force coefficients and with data from full-scale monitoring of the bridge cables.

The aerodynamic damping ratio was determined for two orthogonal directions. The sub-critical Re range was denoted until $Re \approx 1.5 \cdot 10^5$ with a linear increasing damping for the two planes. Hereafter, the out-of-plane damping decreased and regained a positive slope at $Re = 1.8\text{-}2.0 \cdot 10^5$. No instability was found though. In the in-plane direction no significant decrease in damping values was observed. The aerodynamic damping ratio for the out-of-plane direction reached a maximum of $\zeta_a \approx 0.4\%$. The aerodynamic damping in the in-plane direction reached a maximum of $\zeta_a \approx 0.25\%$. The results agreed with analytical estimations, predicting the out-of-plane damping in the ratio 2:1 with the in-plane damping, in the sub-critical Re range. Furthermore, a good agreement with values obtained from full-scale monitoring was found.

Drag coefficients from dynamic tests were observed to be in broad agreement with the coefficients obtained from static tests and the drag crisis correlated with the decrease in damping values. The lift coefficients showed strong similarity over the tested Re range.

Acknowledgments

The current work was conducted in the DTU/FORCE Technology CWT facility, which is funded by Femern A/S and Storebælt A/S.

References

Acampora, A. 2011. Results of the monitoring of the Øresund Bridge for the period from 12/01/2010 to 30/06/2011. *Internal report. CESDyn, DTU Byg.*

Acampora, A., & Georgakis, C.T. 2013. Aerodynamic coefficients of plain and helically filleted twin cylinders for varying wind angles of attack. *Unpublished: submitted to the 6th European and African Conference of Wind Engineering, Cambridge, UK.*

Acampora, A., & Georgakis, C.T. 2011. Recent monitoring of the Øresund Bridge: Observations of rain-wind induced cable vibrations. *In: 13th International Conference of Wind Engineering, Amsterdam, NL.*

Acampora, A., Macdonald, J.H.G., Georgakis, C.T., & Nikitas, N. 2012. Identification of aeroelastic forces on twin bridge cables from full-scale measurements in skewed winds. *In: 10th UK Conference on Wind Engineering, Southampton, UK.*

Cooper, K., Mercke, E., & Wiedemann, J. 1999. Improved blockage corrections for bluff-bodies in closed and open wind tunnels. *In: 10th International Conference Wind Engineering, Copenhagen, DK.*

Georgakis, C.T., & Acampora, A. 2011. Determination of the aerodynamic damping of dry and wet bridge cables from full-scale monitoring. *In: 9th International Symposium on Cable Dynamics, Shanghai, CN.*

Georgakis, C.T., Koss, H.H., & Ricciardelli, F. 2009. Design specification for a novel climatic wind tunnel for testing of structural cables. *In: 8th International Symposium on Cable Dynamics, Paris, FR.*

Gimsing, N. J., & Georgakis, C. T. 2012. *Cable Supported Bridges: Concept and Design*, Third edn. John Wiley & Sons Ltd.

Kleissl, K., & Georgakis, C. T. 2012. Comparison of the aerodynamics of bridge cables with helical fillets and a pattern-indented surface. *Journal of Wind Engineering and Industrial Aerodynamics*, **104-106**, 166–175.

Larose, G.L., & Smitt, L.W. 1999. Rain/wind induced vibrations of the stays of the Öresund High Bridge. *In: 1999* IABSE Conference, *Malmö, SW.*

Macdonald, J.H.G., & Larose, G.L. 2006. A unified approach to aerodynamic damping and drag/lift instabilities, and its application to dry inclined cable galloping. *Journal of Fluids and Structures*, **22**, 229–252.

Macdonald, J.H.G., & Larose, G.L. 2008. Two-degree-of-freedom inclined cable galloping-Part 1: General formulation and solution for perfectly tuned system. *Journal of Wind Engineering and Industrial Aerodynamics*, **96**, 291-307.

Raeesi, A., Cheng, S., & Ting, D. S. K. 2012. Some Insight into the Wind-Induced Vibration of Stay Cables in the Context of Rigid Static Inclined Circular Cylinder. *Journal of Applied Fluid Mechanics*, **5(2)**, 99–112.

Zdravkovich, M.M. 2003. *Flow around circular cylinders. Volume 2: Applications.* First edn. Oxford University Press.